Electronic Supplementary Material (ESI) for Physical Chemistry Chemical Physics.

A new record excited state ^{3}MLCT lifetime for metalorganic iron(II) complexes

Li Liu,[a] Thibaut Duchanois,[b] Thibaud Etienne,[c] Antonio Monari,[c] Marc Beley,[b] Xavier Assfeld,[c] Stefan Haacke,[*a] Philippe C. Gros[*b]

[a] IPCMS & Labex NIE, Université de Strasbourg & CNRS, Rue du Loess, 67034 Strasbourg Cedex, France. stefan.haacke@ipcms.unistra.fr
[b] Université de Lorraine–Nancy & CNRS, HecRIn, SRSMC, Boulevard des Aiguillettes, 54506 Vandoeuvre-Lès-Nancy, France. philippe.gros@univ-lorraine.fr
[c] Université de Lorraine–Nancy & CNRS, HecRIn, SRSMC, Boulevard des Aiguillettes, 54506 Vandoeuvre-Lès-Nancy, France.

Supporting Information

Table of Contents

^{1}H and ^{13}C NMR spectra of ligands and complexes

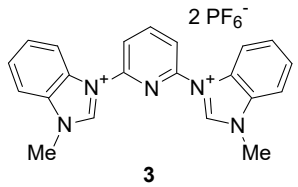

3

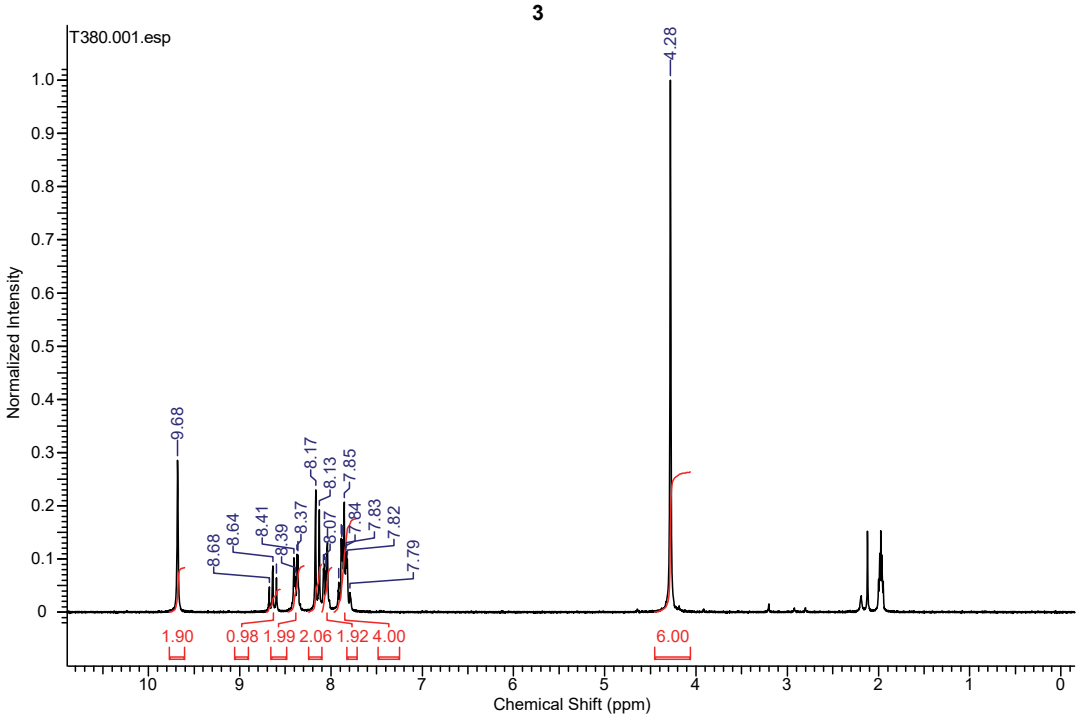

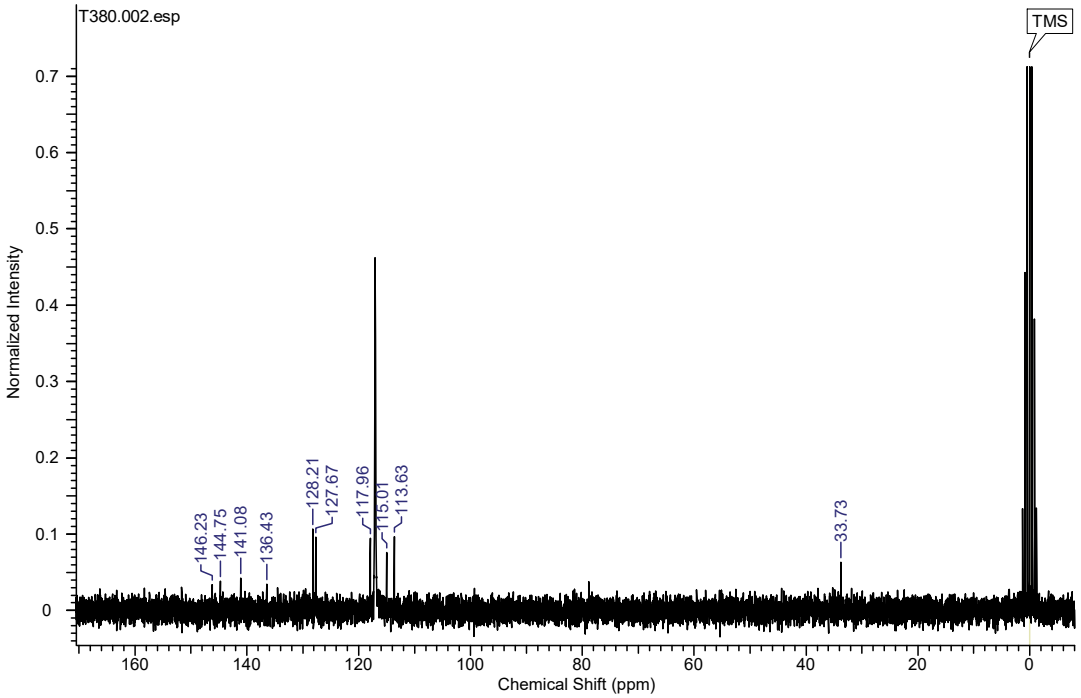

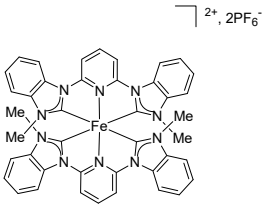
2+, 2PF6-
Me
Me
Fe
Me
Me

C3

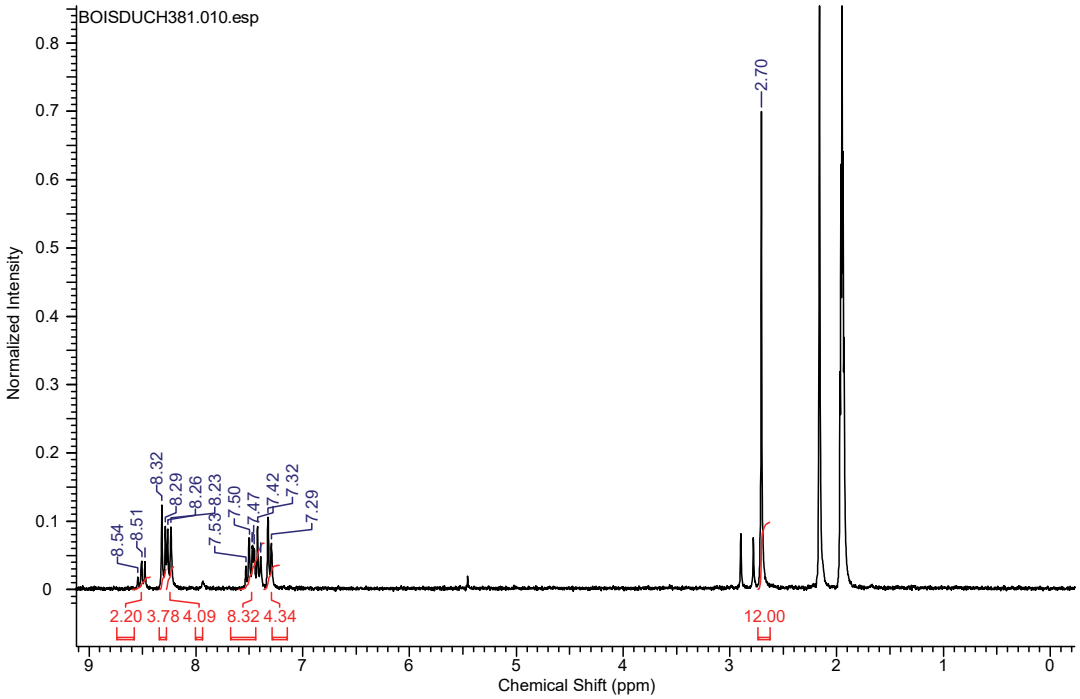
BOISDUCH381.010.esp
Normalized Intensity
Chemical Shift (ppm)
8.54
8.51
8.32
8.29
8.26
8.23
7.53
7.50
7.47
7.42
7.32
7.29
2.70
2.20
3.78
4.09
8.32
4.34
12.00

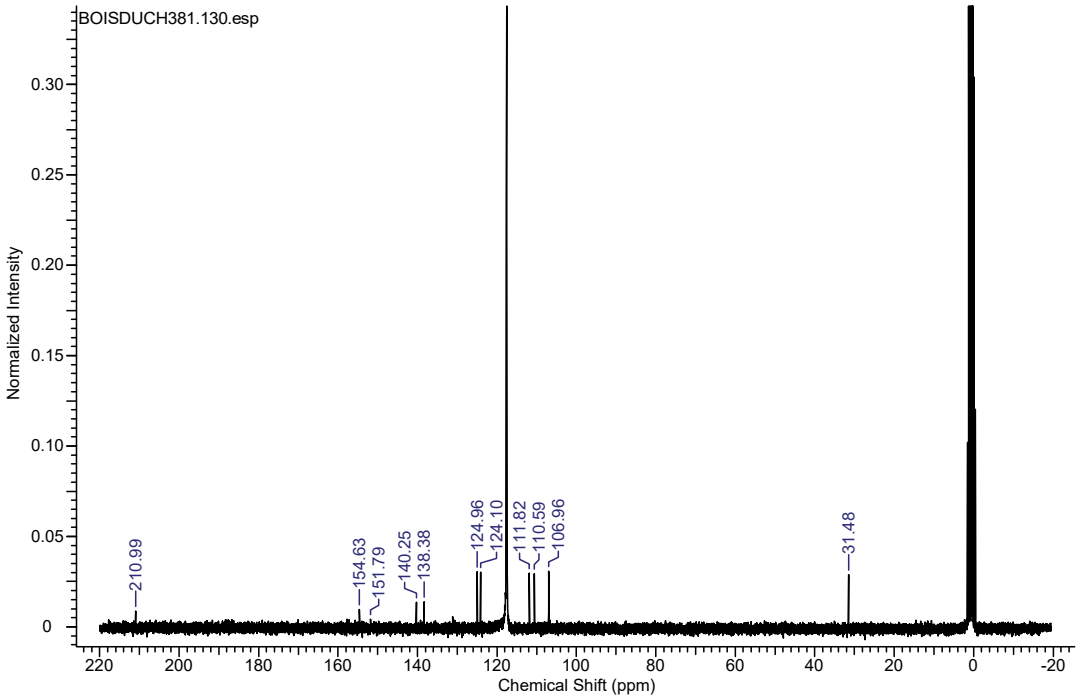
BOISDUCH381.130.esp
Normalized Intensity
Chemical Shift (ppm)
210.99
154.63
151.79
140.25
138.38
124.96
124.10
111.82
110.59
106.96
31.48

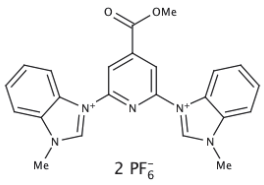
O
OMe
N+
N
N+
N
Me
Me
2 PF6−

4

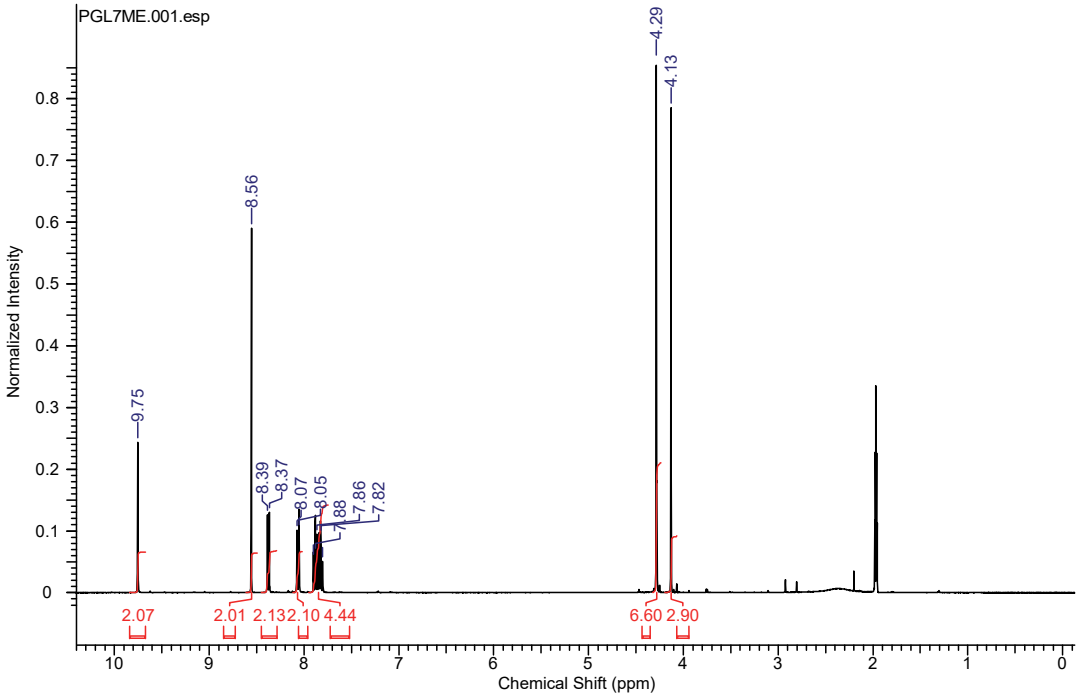
PGL7ME.001.esp
Normalized Intensity
Chemical Shift (ppm)
9.75
8.56
8.39
8.37
8.07
8.05
7.88
7.86
7.82
4.29
4.13
2.07
2.01
2.13
2.10
4.44
6.60
2.90

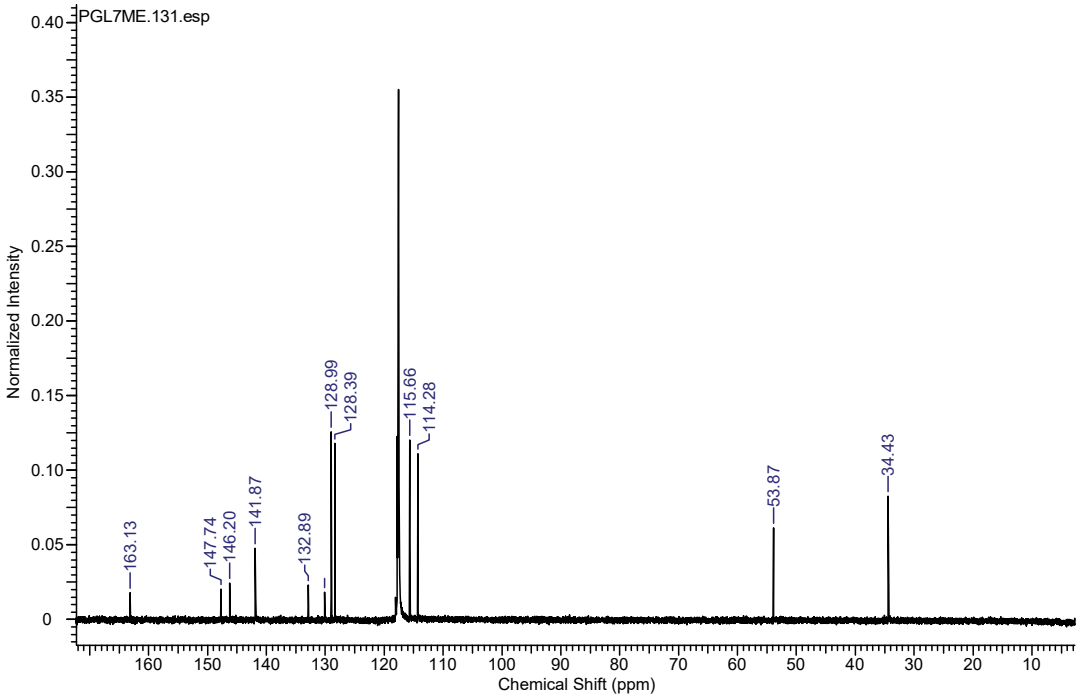
PGL7ME.131.esp
Normalized Intensity
Chemical Shift (ppm)
163.13
147.74
146.20
141.87
132.89
128.99
128.39
115.66
114.28
53.87
34.43


2 PF6

C4

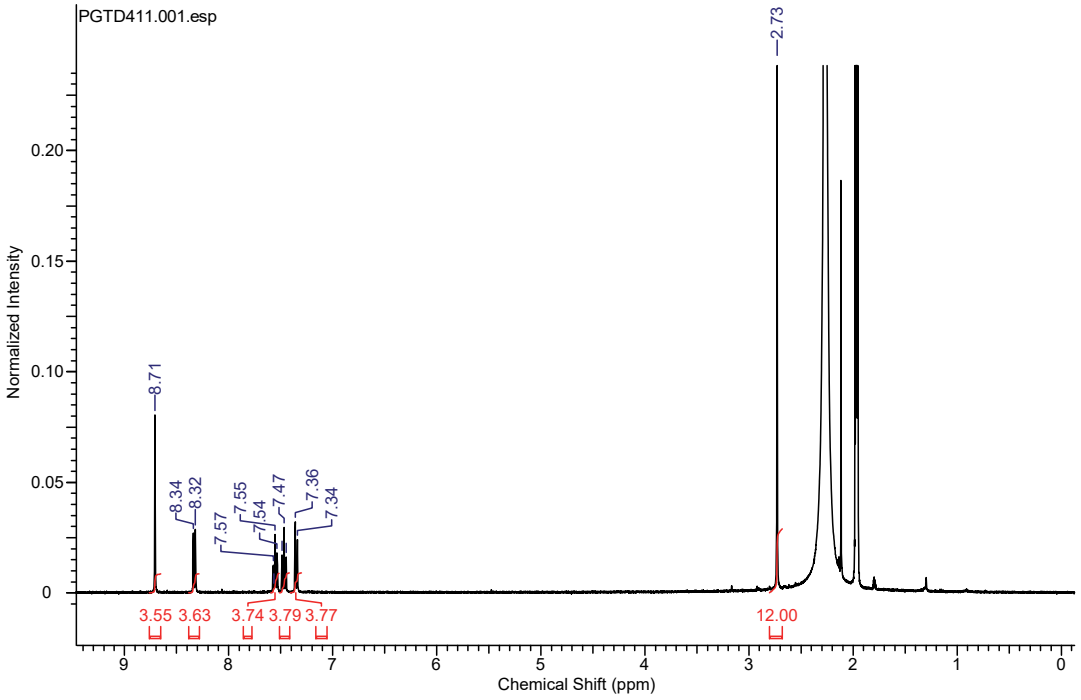
PGTD411.001.esp
Normalized Intensity
Chemical Shift (ppm)
8.71
8.34
8.32
7.57
7.55
7.54
7.47
7.36
7.34
2.73
3.55
3.63
3.74
3.79
3.77
12.00

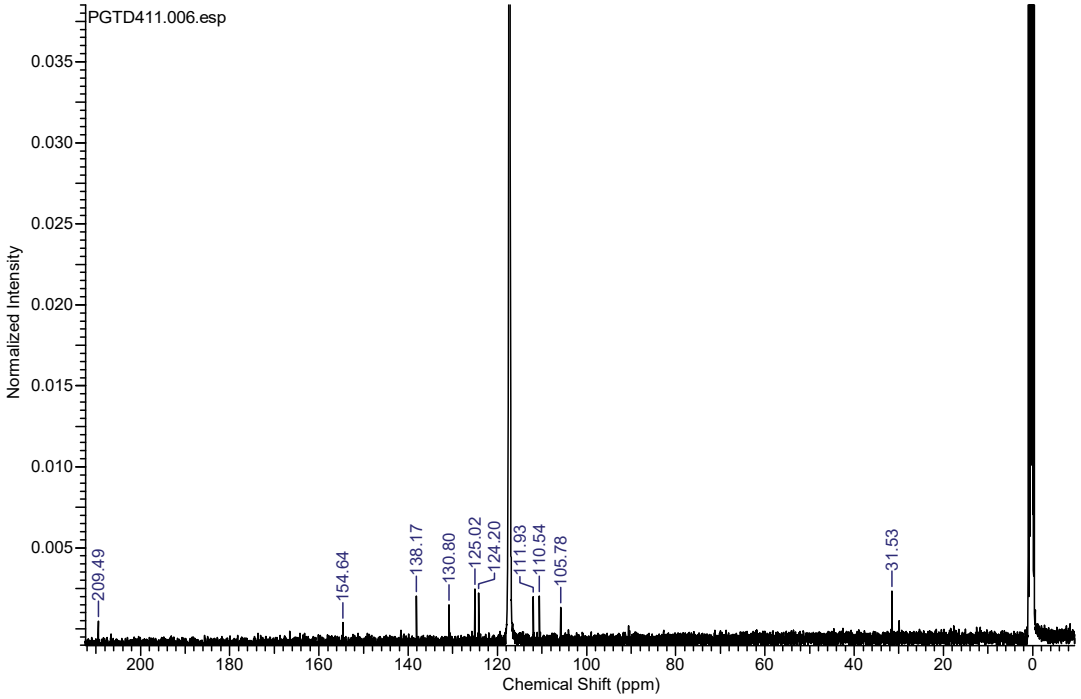
PGTD411.006.esp
Normalized Intensity
Chemical Shift (ppm)
209.49
154.64
138.17
130.80
125.02
124.20
111.93
110.54
105.78
31.53

Photophysics

Singular Value Decomposition (SVD) and Decay Associated Spectra (DAS)

As described previously, the SVD, as Eq1, is applied to the transient absorption spectroscopy data after chirp and solvent correction. [Briand] In order to reduce noise level, the five first kinetic traces are involved to be taken to analyze as shown in the Fig S1. (symbol lines, black square for the first, red round for the second, blue up triangle for the forth and green diamond for the fifth) They are fitted by a sum of one Gaussian and bi-exponential function with same time constants as Eq2 and different amplitudes as the solid lines in the Fig S1 as the respective colors. Obviously, the first component (TR1) contains the majority of information, especially the long-lived component. And the third component (TR3) also has a great contribution for the fast component(s). The table S1 presents the fitting parameters. The DAS are reconstituted by those fitted amplitudes as Eq 3 with U vectors shown in Fig 2(B).

$$\boldsymbol{\Delta A(\lambda,t) = \sum_{s_i} \varepsilon_{s_i}(\lambda)\Delta C_{s_i}(t)L = u(\lambda) * S * v(t) = u(\lambda) * Tr(t)} \textbf{ (Eq.1)}$$

$$\boldsymbol{TR_j(t) = \sum(A_{1,j} * G(\tau) + A_{2,j}exp(-k_2 t) + A_{3,j}exp(-k_3 t))} \textbf{ (Eq.2)}$$

$$\boldsymbol{DAS_i(\lambda) = \sum A_{i,j}u_j(\lambda)} \textbf{ (Eq.3)}$$

	τ	TR1	TR2	TR3
DAS1	<IRF	-0.275	0.001	-0.029
DAS2	65fs	0	-0.008	0
DAS3	27ps	-1.278	0.042	0

Table S1. Fitting parameters of **C4**

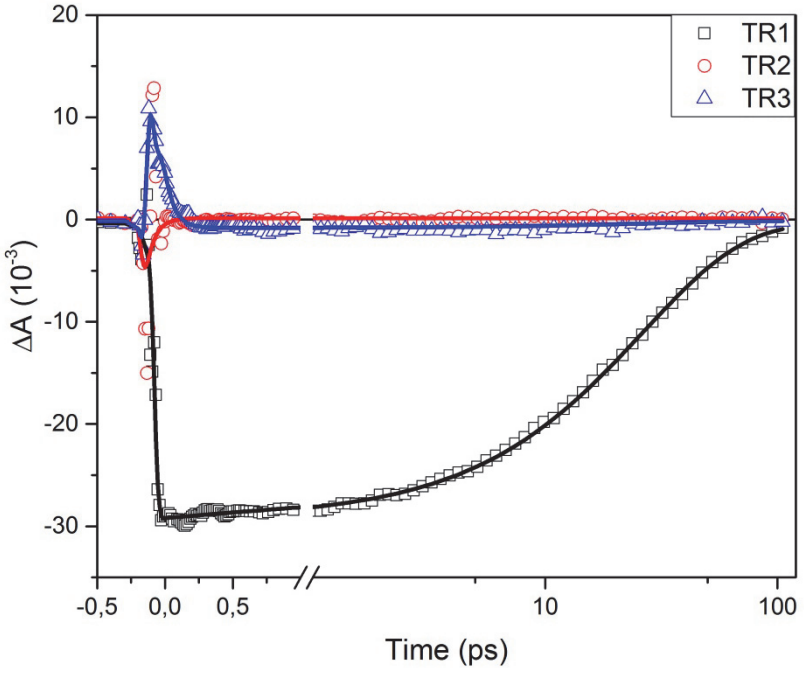

Fig S1. The three first components (symbol lines) of transient absorption spectroscopy data singular value decomposition (SVD) with their fits (solid lines)

Excited state relaxation and thermalization

Figure S2 shows the evolution of differential spectra (Figure S2A and S2C) and kinetic traces (Figure S2B) of C3 in acetonitrile upon excitation at 480nm. In the first 400fs, the spectral narrowing and the blue-shift in the red part

are more pronounced than for C4 (Figure 4A). The peak of ESA in the region above 500 nm is shifted from 600 nm at 40fs (black curve), to near 500 nm at 440 fs (pink curve). Meanwhile, the other ESA bands rise at 350 and 400 nm and undergo spectral changes, as the high energy peak at 350-370 nm increases relatively to the one at 390-400 nm. Note that this ESA is partly reduced by GSB (Figure 2). Indeed, at 40 fs delay, amplitudes of ESA and GSB are almost the same as the ΔA signal is nearly zero in the near-UV. Due to excited state thermalization the near-UV ESA band appears, on the same time scale as the spectral changes in the 550 to 650 nm range. These spectral changes, due to excited state relaxation and thermalization, are best reflected in the initial sub-ps decay and the rise of the kinetic traces at 649nm (black) and 449nm (pink curve) in Figure S2B.

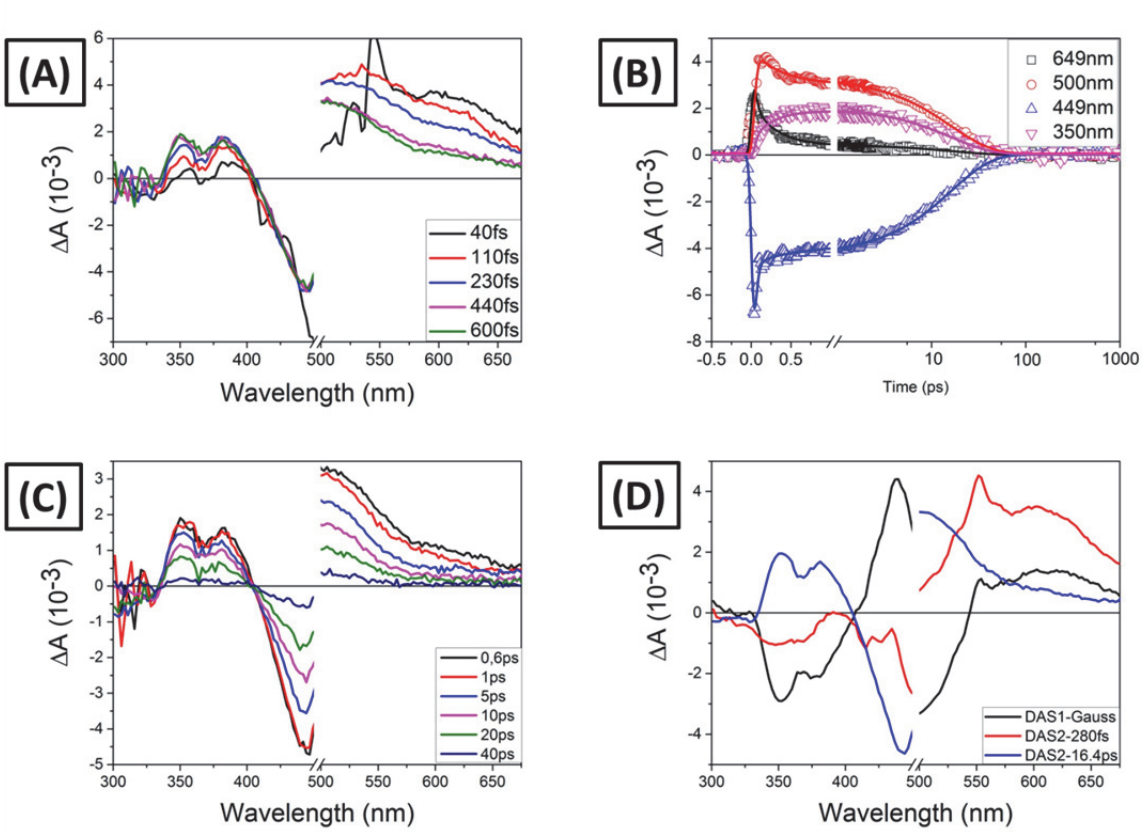

Fig S2. Selected transient differential spectra of C3 in MeCN excited at 480 nm at t <600 fs (A) and at t<40ps(C), kinetic traces (open symbols) with their fits (solid lines) (B) and Decay-Associated differential Spectra (D). As the new formed ESA between 350 nm and 450 nm in (A) and the over-cross of kinetic traces between 650nm and 450 nm in (B), it's much clearer that the blue spectral shift of ESA within 500 fs, which implies the thermalized state. The peaks at 550 nm and 530 nm are stimulated Raman signals.

In Figure S2C, after 0.6ps, the long-lived spectra only delay without any spectral feature change. The board ESA bands show the similar spectral feature as ^{3}MLCT state of C4. (See paper) The GA indicates that the reaction is the same as described in the paper, ^{1}MLCT→thermalization state(s)→^{3}MLCT, as DAS shown in Figure S2D.

Protonation and Deprotonation of C2.

In order to confirm the prolonged ^{3}MCLT by carboxylic group, effect of deprotonation is investigated as function of pH. One drop of high concentration HCL (37% sigma-aldrich) or of high concentration NaOH (2M in H_2O) is added in 50ml pure MeCN to form proton or deproton in C2. With the high pH, the steady-state absorption, shown in Figure S3, has a 40nm blue shift due to negatively charged COO^- termination. Figure S4 illustrates the evolution of differential spectra ((A)-(F)) at <1ps ((A)-(C)) and until 30ps ((D)-(F)) and Decay-Associated differential Spectra ((G)-(I)) as low pH (MeCN-HCL, (A),(D),(G)), neutral MeCN ((B),(E),(H)) and high pH (MeCN-NaOH, (C),(F),(I)). While decreasing the pH by adding the HCL, differential spectra ((A),(B),(D),(E)) and kinetics traces ((G),(H) and also shown in Figure S5) have no significant change. Only the thermalization state has a slightly short lifetime (87fs in MeCN-HCL vs 130fs in MeCN) since it depends on the environment. With the high pH, the differential spectra have similar spectral feature as a board ESA band above 550nm, two narrow ESA bands around 330nm and 425nm. Due to the blue shift of GSB, the ESA around 425nm is recovered. However, the spectral feature is

still obvious. The GA with same fitting function (one Gaussian and two exponential decays) is applied to identify different states as described previously and in the paper. The ^{3}MLCT state lifetime is reduced to 14.5ps with high pH. (16.5ps in low pH and neutral MeCN) Since negatively charged COO^- termination replaces the neutral carboxylic group, the reduced lifetime is expected as the charge would localize near the metal center.

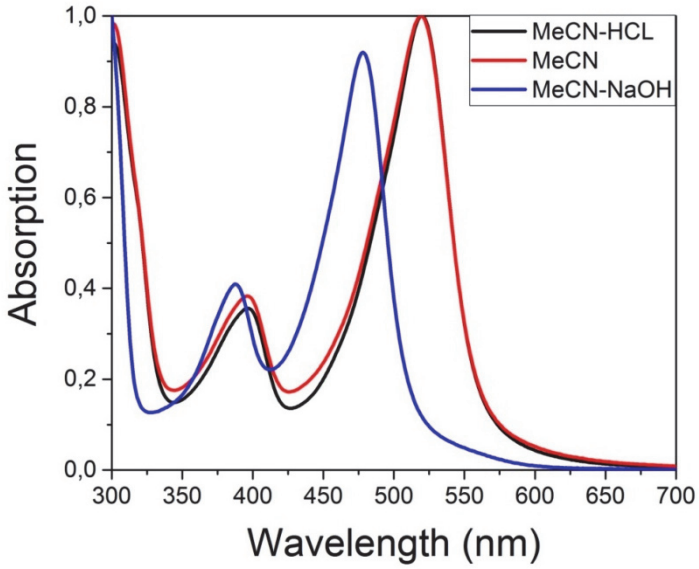

Figure S3. Steady-state absorption of C2 with low pH (MeCN-Hcl), pure MeCN and high pH (MeCN-NaOH). The high pH MeCN has effect of deprotonation with 40nm blue shift.

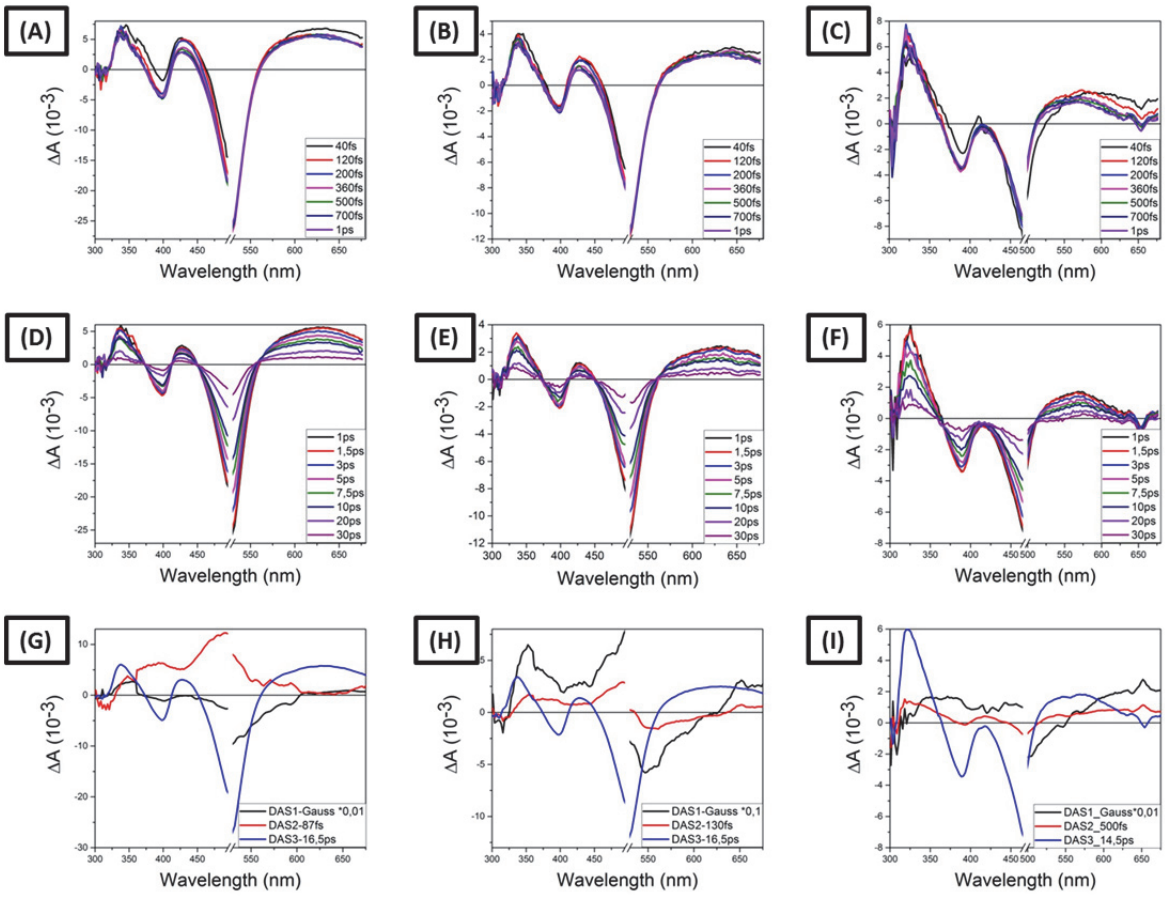

Figure S4. The evolution of differential spectra ((A)-(F)) at <1ps ((A)-(C)) and until 30ps ((D)-(F)) and Decay-Associated differential Spectra ((G)-(I)) as low pH (MeCN-HCL, (A),(D),(G)), neutral MeCN ((B),(E),(H)) and high pH (MeCN-NaOH, (C),(F),(I)). The ^{3}MLCT state lifetime is reduced to 14.5ps with high pH due to negatively charged COO^- termination.

Kinetic traces of ESA, normalized at 1ps in different pH MeCN are shown in Figure S5 with their fits. The fitting parameters are same as GA in Figure S4. The 3MLCT lifetime is same in the MeCN and MeCN-HCL as 16.5ps and is reduced to 14.5ps as COO^- formed.

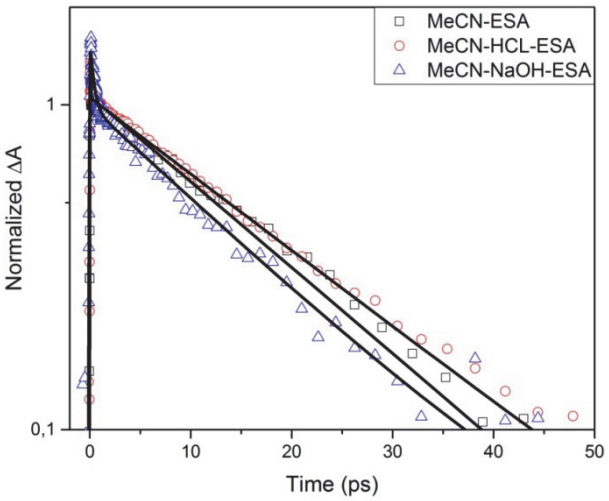

Figure S5. Kinetic traces (open symbols) of C2 in MeCN (black square), MeCN-HCL (red circle) and MeCN-NaOH (blue triangle) normalized at 1ps with their fits (black lines, same parameters as shown in Figure S2). The ^{3}MLCT state lifetime is reduced to 14.5ps with high pH due to negatively charged COO^- termination.

Molecular Modeling and Simulations

All quantum chemistry calculations were performed by using the Gaussian09 suite of programs. The ground-state geometry off all the complexes have been optimized at the DFT level by using the B3LYP exchange correlation functional. The double-z LANL2DZ basis set was used for the iron atom, whereas carbon, hydrogen, and nitrogen were describedby using the 6-31+G(d,p) basis set. Singlet excited states were firstly obtained as vertical transitions from the equilibrium geometry, following the usual Franck-Condon approach, at TD-DFT level. In this case the system was described using HCTCH exchange correlation functional, and the 6-31+G(d,p) basis set for all the atoms. Note that these conditions have been chosen as the ones that better reproduce the lowest energy part of the absorption spectrum relative to the experimental one.

In all the calculations solvent effects were taken into account by using the polarizable continuum model (PCM); more specifically, acetonitrile was considered throughout. The density reorganization in the excited

states was analyzed in terms of NTOs by using a locally produced and free downloadable code NancyEX (see www.nancyex.sourceforge.net/).

Once the singlet states assessed the same level of theory was used to investigate the triplet manifold, triplet nature (MC or MLCT) was easily identified using the NTO analysis. Subsequently, the first 3MLCT and the first 3MC have been optimized, again with TDDFT at HCTCH/6-31+G(d,p) level of theory, in order to obtain the adiabatic relaxation energies.

Finally f_S values have been obtained once again using the NancyEX code from a post-processing of the attachment and detachment densities. For the reader convenience we recall that f_s is based on the normalized overlap of the detachment and attachment densities, calculated in the direct space. As such values close to 1.0 are indicative of localized transitions, while charge-transfer states are characterized by values close to zero. The lower the value of f_s the higher is the charge-transfer nature of the state.